New Phytologist

Research

Conifers depend on established roots during drought: results from a coupled model of carbon allocation and hydraulics

D. Scott Mackay[1], Philip R. Savoy[2], Charlotte Grossiord[3], Xiaonan Tai[1], Jonathan R. Pleban[1], Diane R. Wang[1], Nathan G. McDowell[4], Henry D. Adams[5] and John S. Sperry[6]

[1]Department of Geography, University at Buffalo, Buffalo, NY14261, USA; [2]Department of Biology, Duke University, Durham, NC 27708, USA; [3]Swiss Federal Institute for Forest, Snow and Landscape Research WSL, Zürcherstrasse 111, 8903, Birmensdorf, Switzerland; [4]Pacific Northwest National Laboratory, Richland, WA 99354, USA; [5]Department of Plant Biology, Ecology, and Evolution, Oklahoma State University, Stillwater, OK 74078, USA; [6]Department of Biology, University of Utah, Salt Lake City, UT 84112, USA

Author for correspondence:
D. Scott Mackay
Tel: +1 716 645 0477
Email: dsmackay@buffalo.edu

Received: *5 February 2019*
Accepted: *1 July 2019*

New Phytologist (2020) **225:** 679–692
doi: 10.1111/nph.16043

Key words: carbon allocation, drought, fine roots, hydraulics, simulation, trees, warming.

Summary

- Trees may survive prolonged droughts by shifting water uptake to reliable water sources, but it is unknown if the dominant mechanism involves activating existing roots or growing new roots during drought, or some combination of the two.
- To gain mechanistic insights on this unknown, a dynamic root-hydraulic modeling framework was developed that set up a feedback between hydraulic controls over carbon allocation and the role of root growth on soil–plant hydraulics. The new model was tested using a 5 yr drought/heat field experiment on an established piñon-juniper stand with root access to bedrock groundwater.
- Owing to the high carbon cost per unit root area, modeled trees initialized without adequate bedrock groundwater access experienced potentially lethal declines in water potential, while all of the experimental trees maintained nonlethal water potentials. Simulated trees were unable to grow roots rapidly enough to mediate the hydraulic stress, particularly during warm droughts. Alternatively, modeled trees initiated with root access to bedrock groundwater matched the hydraulics of the experimental trees by increasing their water uptake from bedrock groundwater when soil layers dried out.
- Therefore, the modeling framework identified a critical mechanism for drought response that required trees to shift water uptake among existing roots rather than growing new roots.

Introduction

Global climate dynamics are causing more frequent and widespread tree die-offs as a result of extreme droughts and higher temperatures (Adams *et al.*, 2009; Williams *et al.*, 2013; McDowell *et al.*, 2016). Ability to access water from reliable sources, such as groundwater stored in bedrock fractures (McLaughlin *et al.*, 2017), is one strategy some trees may use to survive in a warmer world with intense droughts. This is especially critical in situations of scarce precipitation (Tai *et al.*, 2018). Plants must grow coarse root systems towards groundwater (Fan *et al.*, 2017) and maintain sufficient absorbing fine roots to acquire the groundwater. Studies suggest that plants in drought-prone regions maintain roots specifically for accessing alternative water sources when precipitation is scarce (Dawson, 1993; Burgess *et al.*, 1998; Jackson *et al.*, 1999; Rose *et al.*, 2003; Eberbach & Burrows, 2006; David *et al.*, 2007; Bleby *et al.*, 2010; Miller *et al.*, 2010; Pinheiro *et al.*, 2016; Grossiord *et al.*, 2017a; Johnson *et al.*, 2018). But the construction of roots carries energy costs, including the use of net primary production of carbon (C). Development of larger root systems requires a notable alteration of C allocation between above-ground and below-ground organs, in what appears to be a coordinated process (Hacke *et al.*, 2000; Magnani *et al.*, 2002; Li & Bao, 2015). Changes in biomass partitioning probably reflect long-term adjustments or species adaptations to available water (Grier & Running, 1977; Gholz, 1982; Kozlowski & Pallardy, 2002; Hartmann, 2011) to maintain hydraulic health within the constraints of available C resources (Johnson *et al.*, 2013; Mencuccini *et al.*, 2015). Vegetation models have profited from some of this theory to account for C allocation to roots and leaf area (Fisher *et al.*, 2018), but they do not yet integrate these dynamics with hydraulics. Thus, model development should relate C allocation to fine root and leaf areas, as these are both hydraulically important (Sperry *et al.*, 2002; Comas *et al.*, 2013).

Fine roots may play both passive and active roles in plant hydraulic status. Plant hydraulic models with segmented root systems (Sperry *et al.*, 1998, 2016; Mackay *et al.*, 2015) currently simulate proportional changes in water uptake from different parts of the root system as a passive response to hydraulic gradients without a need for an active response once the fine (absorbing) and coarse (transport) root system is established. But the active role of fine roots during drought has also been observed. Early onset of mechanical failure of cortical cells (Cuneo *et al.*, 2016)

and the ability of some species to disconnect their fine roots from the soil under water deficit (West *et al.*, 2007a,b; Plaut *et al.*, 2013) suggest that fine roots act as hydraulic fuses (Venturas *et al.*, 2017). Control of aquaporins or changes in fine root area can also cause adjustments to hydraulic conductance (Gambetta *et al.*, 2012; Venturas *et al.*, 2017). To account for these active roles of fine roots, models need to define fine roots in a way that is meaningful for quantifying water uptake (McCormack *et al.*, 2015) and integrate plant hydraulic status with a C-mediated growth strategy (Fisher *et al.*, 2018; Hartmann *et al.*, 2018).

Two challenges in building models that integrate both active and passive root functions are the apparently contradictory root growth responses to drought and the large variability in root traits that yield similar function. Consider the first challenge. Fine root production has been shown to increase with decreasing water availability (Gower *et al.*, 1992; Ewers *et al.*, 2000; Barnes, 2002; Kozlowski & Pallardy, 2002; Hertel *et al.*, 2013). Yet observed fine root biomass has also declined during drought (Joslin *et al.*, 2000; Meier & Leuschner, 2008; Ruehr *et al.*, 2009; Anderegg, 2012; Moser *et al.*, 2014), probably as a result of various factors, including a decline in net production and an increase in mortality (Aaltonen *et al.*, 2016). Other studies found negligible changes in root growth during seasonal or long-term periods of soil water deficit (Metcalfe *et al.*, 2008; Barbeta *et al.*, 2015; Doughty *et al.*, 2014), suggesting that trees rely heavily on existing roots during drought. The role of a stratified root architecture having access to reliable water during drought provides a better explanation for tree survival than root : shoot ratios or biomass allocation (Padilla & Pugnaire, 2007; Laclau *et al.*, 2013; Doughty *et al.*, 2014), but just how much deep root area is needed is unknown. One observation that can be made from these studies is that the maintenance of roots near stable water sources reduces the need to grow new roots after the onset of drought.

The second challenge to building integrated models of C allocation and hydraulics is that each unit investment of C can yield different water-uptake capacities (Reich *et al.*, 1998; Bauhus & Messier, 1999; Withington *et al.*, 2006; Bowsher *et al.*, 2016; Kramer-Walter *et al.*, 2016) associated with phylogenetic variations (Comas *et al.*, 2002, 2014; Comas & Eissenstat, 2009; Ma *et al.*, 2018). In particular, the finest root diameters show a large variability among taxa, soil textures and climates (Eissenstat *et al.*, 2015; Cheng *et al.*, 2016; Liu *et al.*, 2016). For example, first-order (or finest) roots in subtropical areas can be thicker because of favorable conditions for water uptake (Chen *et al.*, 2013), whereas temperate trees generally have thinner first-order roots (Pittermann *et al.*, 2012). In turn, this results in different water-uptake capacities per unit C invested. Two widely measured traits, specific root length, a measure of root length per unit C invested, and first- and second-order root diameters, are potentially useful here because together they define root tissue density (Ostonen *et al.*, 2007; Ma *et al.*, 2018; see also Supporting Information Fig. S1). Root tissue density informs the C allocation needed per unit increment of root volume and, by implication, of root area. Notably, evergreen needleleaf tree root tissue densities are high relative to other taxa, as they have low specific root areas across a wide range of diameters (Fig. S1). Thus, a second observation is that specific root length and root diameter can potentially be utilized along with the observation that optimal water transport is observed when root xylem and rhizospheres are colimiting (Sperry *et al.*, 2002) to provide a robust link between C allocation and hydraulics.

Here we present a new modeling framework that addresses the first issue regarding variability in observed root growth responses to drought by allowing for transience in root growth in a feedback with the plant hydraulic system, and addresses the second issue in variation in root traits by representing the fine root system with a small number of measurable traits that can be used to translate C allocation into absorbing root area. We make no assumptions about root trait correlations, and instead allow the integrated dynamics of C allocation and hydraulic function to be an emergent response to environmental conditions. Our objective is to add mechanistic insight on fine root dynamics, associated C costs, and their integration with rhizosphere–plant hydraulics, specifically during hot and dry conditions. We tested the framework at a piñon-juniper site with empirical evidence of root water uptake from bedrock fractures and strong tree resistance to droughts, including warmer droughts (Grossiord *et al.*, 2017a). To focus this study, we use the new framework to test two hypotheses: (H1) trees rely on bedrock groundwater during dry periods and soil water during wetter periods to maintain their hydraulic status; and (H2) fine roots with access to bedrock groundwater must be maintained at all times rather than grown after the onset of drought.

Materials and Methods

Study site description

This study was conducted at the Los Alamos Survival-Mortality (SUMO) experiment in New Mexico, USA (35.49°N, 106.18°W, 2175 m asl). The soil is Hackroy clay loam, which is derived from volcanic tuff (Soil Survey Staff, Natural Resources Conservation Service, United States Department of Agriculture; http://websoilsurvey.nrcs.usda.gov), with an average depth of 65 cm. The volcanic tuff at the site is fractured (Trainer, 1974), which allows tree roots to grow into the bedrock (Tierney & Foxx, 1982; Newman *et al.*, 1997). Calcite precipitation in the near-surface fractures induced by root growth and decay (Newman *et al.*, 1997) and isotopic signatures showing SUMO trees using water from below the soil layer (Grossiord *et al.*, 2017a) support tree root access to groundwater within its seasonal range of depths within the bedrock fractures. We do not know if the bedrock water uptake is by roots alone or if it is facilitated by mycorrhizas. The dominant tree species are piñon pine (*Pinus edulis* Engelm.) and one-seed juniper (*Juniperus monosperma* (Engelm.) Sarg.). Intercanopy spaces also contain a small amount of biomass in grass, cacti and Gambel oak. The 0.4 ha experimental site is surrounded by piñon that died during a 2002–2003 drought. Mean annual temperature is 10.1°C and mean annual precipitation is 360 mm (1987–2016 mean), with *c.* 50% falling during the North American Monsoon season from July to September (http://environweb.lanl.gov/weathermachine).

In June 2012, open-top chambers holding air temperature at *c.* 4.8°C above ambient and clear polymer troughs that excluded 45% of precipitation were installed to establish heat, drought, drought + heat, and untreated (or ambient) treatments for both piñon and juniper. In April 2016, the trough coverage of the drought and drought + heat structures was increased to 90% to simulate extreme drought conditions (Grossiord *et al.*, 2017b). Each species treatment had five to six trees with tree ages of 56 ± 5 and 79 ± 7 yr for piñon and juniper, respectively, determined from increment cores, and heights between 1.5 and 4.5 m. Micrometeorological conditions were measured continuously and recorded by two weather stations at the site (Climatronics, Bohemia, NY, USA). Atmospheric temperature and relative humidity were measured in all chambers using C215 Campbell sensors (Campbell Scientific, Logan, UT, USA) at two positions (1 m height and two-thirds of canopy height), and used for controlling industrial-scale air-conditioning units that regulated chamber temperature. No tree mortality occurred over the full study period (2012–2016). More details on the study site are provided in Adams *et al.* (2015).

Model development

The new modeling framework was integrated into Trees (Mackay *et al.*, 2015), which computes soil–plant hydraulics, photosynthesis, canopy diffusive conductance (stomatal, boundary), respiration, and nonstructural C (NSC). Trees has been well tested to show that it can predict seasonal time series of leaf water potentials, soil water content, and canopy transpiration with input of hydraulic parameters from a single day (Mackay *et al.*, 2015; Tai *et al.*, 2017; Johnson *et al.*, 2018). It is forced with observed meteorological data (temperature, wind speed, vapor pressure deficit, photosynthetically active radiation, and precipitation), and constrained with measured parameters on hydraulics, gas exchange, allometry, and root structure. Trees retains a memory of cavitation in each xylem segment, which means the maximum hydraulic conductance declines with successive droughts. Hydraulic conductance values can be recomputed from soil water potential if observed plant hydraulic status (e.g. leaf water potentials) supports a post-drought recovery (Mackay *et al.*, 2015).

In the original modeling framework, root area per unit ground area was defined in each soil-root layer as a fixed multiple of leaf area index (LAI). LAI was dynamic, based on the allocation of C to the canopy and a simple leaf area phenology routine (Savoy & Mackay, 2015), but root area was computed by multiplying LAI by a constant root-to-leaf area scalar (Mackay *et al.*, 2015). Carbon allocation throughout the plant was coordinated with whole-plant hydraulic conductance, k_P. If k_P was < 50% of its saturated value, then growth allocation declined at a greater than linear rate and maintenance respiration declined at a linear rate. Here we replaced the constant root-to-leaf area scalar with transient root area computed as a function of C allocated to fine roots and the hydraulic status of each soil-root layer. Details of this new model are discussed in the following.

Root architectures are branching networks (Fig. 1a), in which the two finest root orders (i.e. first order is the finest) account for most of the absorbing root area (McCormack *et al.*, 2015). A branching network is cumbersome to model without detailed below-ground observations, and so here we represent the root system as a series of root layers assuming well-mixed soil water content in each layer (Fig. 1b). Each layer was defined as a vector of root orders, represented as cylinders (Fig. 1c), with orders ranging in diameter from low (first order) to high (n^{th} order). The soil-root volume was organized into m layers, each with a vertical thickness given by an input root axial length, L_{ax}, and horizontal extent defined by a lateral root length, L_{lat}. The volume of soil occupied by the root system (Fig. 1b) was computed as:

$$V_{\text{R}} = \pi\left(1 - \frac{\rho_{\text{bulk}}}{\rho_{\text{max}}}\right)\sum_{j=1}^{\text{m}} L_{\text{lat}_j}^2 L_{\text{ax}_j} \qquad \text{Eqn 1}$$

where ρ_{bulk} is soil bulk density (g cm^{-3}) and ρ_{max} is the maximum density ($2.65\ \text{g cm}^{-3}$). For example, a soil-root layer with axial and lateral root lengths of 0.1 m and 1.0 m, respectively, and a soil bulk density of $1.325\ \text{g cm}^{-3}$, has a pore volume of $0.157\ \text{m}^3$.

We assumed root diameter scales linearly with increasing root order between the first-order root and the root collar. Each soil-root layer contained a vector of n (= 10) root orders of diameter, $d_{\mathbf{R}}$, with a range defined between a minimum diameter parameter, d_{min} (mm) and a maximum diameter parameter, d_{max} (mm), of the root collar or tap root. The diameter of each root order was computed as:

$$d_{\text{R}_k} = d_{\text{min}} d_{\text{Rmult}}^{k-1} \qquad \text{Eqn 2}$$

where $d_{\text{Rmult}} = \left(\frac{d_{\text{max}}}{d_{\text{min}}}\right)^{\frac{1}{n-1}}$ is the ratio of the diameter of the k^{th} root order to the diameter of the $(k-1)^{\text{th}}$ root order. A root collar diameter of 40.0 mm and minimum root diameter of 0.125 mm yields $d_{\text{R}} = (0.125, 0.237, \ldots, 40.0)$ mm.

Total root surface area per unit ground surface area, A_{R} (m^2 root m^{-2} ground area), was computed from the amount of root C, $\boldsymbol{C}_{\text{R}}$ (g C m^{-2} ground area), through a linear relationship between root length and root C, given by specific root length, l_{rs} (m g^{-1} C). Total root area for a plant was computed as the summation of the root areas over all layers and root orders, assuming that each j, k root had the surface area equivalent of the cylinder (Fig. 1c) defined by the root circumference times its length,

$$A_{\text{R}} = \pi\sum_{j=1}^{\text{m}}\sum_{k=1}^{\text{n}} l_{\text{rs}_k} \mathbf{C}_{\text{R}_{jk}} d_{\text{R}_k} \qquad \text{Eqn 3}$$

where $l_{\text{rs}_k} = \frac{l_{\text{rs}_1}}{d_{\text{Rmult}}^{2k-2}}$ and l_{rs_1} were obtained empirically from fine root length divided by dry mass of typically the finest one or two root orders. Note also that root tissue density (or C cost per unit root volume) can be computed as $\left(d_{\text{R}_k} l_{\text{rs}_k}\right)^{-1}$ (Ostonen *et al.*, 2007) with appropriate unit conversions. Assuming root dry biomass is 50% C, then if l_{rs_1} is $200\ \text{m g}^{-1}$ C, d_{min} is 0.125 mm, d_{max} is 40 mm, and each root order is allocated $10\ \text{g C m}^{-2}$ ground area, the root area sequence would be (0.785, 0.414,

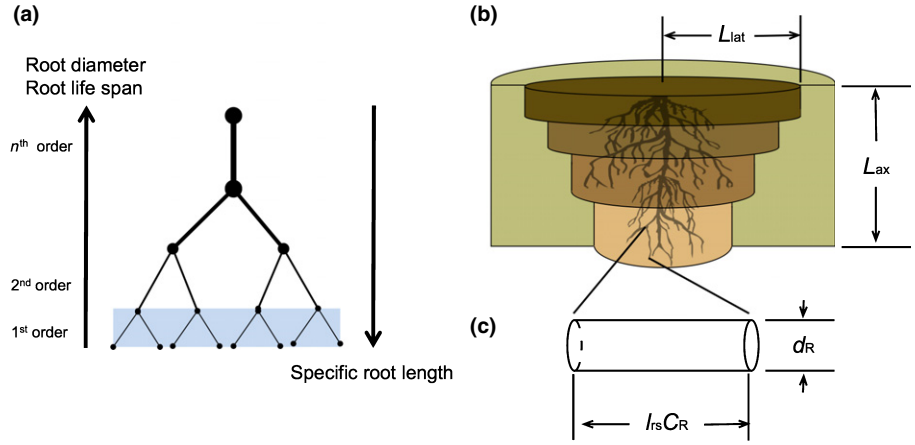

Fig. 1 A simple conceptual model of a branching root system (a) with lower-order roots representing fine roots. By summing all lengths within each respective order, the branching system can be simplified into a vector of root orders, each with a quantifiable specific root length, root diameter and root life span. A vector of root orders is associated with each soil-root layer (b) with axial (L_{ax}) and lateral lengths (L_{lat}). (c) For each root order, the surface area of a cylinder defines the order's contribution to absorbing root area, given carbon content ($\boldsymbol{C}_R$), specific root length (l_{rs}) and diameter (d_R).

0.218, . . ., 0.0025) m^2 root area m^{-2} ground area. In this example, the first three root orders comprise 86% of A_R. The value of d_{max} may not be readily available from data, and so it is useful to note that with 10 root orders the contribution to A_R from the first three orders is insensitive to d_{max}, especially for values > 20 mm.

Carbon for growth and maintenance is taken from net photosynthesis loaded into a pool of NSC. Maintenance respiration is taken from NSC before calculation of growth allocation, as explained in Mackay *et al.* (2015). Here the response rate of maintenance respiration to temperature was linearly scaled from the root value in the first-order roots to the stem rate in the 10th-order roots to yield comparatively higher maintenance costs in finer roots (Pregitzer *et al.*, 1998; Makita *et al.*, 2012). Root area dynamics were integrated with C allocated to roots, $\boldsymbol{C}_R$, with the following simple first-order equation with respect to time t:

$$\left(\frac{dA_R}{dt}\right)_{jk} = \left(\frac{d\mathbf{C}_R}{dt}\right)_{jk} \pi d_{R_k} l_{rs_k} \qquad \text{Eqn 4}$$

The rate of change of C in each root represents a balance between the allocation of new C and root mortality. We assumed that the allocation of new C to each soil-root layer was proportional to the hydraulic health of the respective layers. This is supported by empirical evidence of declining root growth with soil water potential (Teskey & Hinckley, 1981), patchy root growth associated with areas of higher soil water (Hendrick & Pregitzer, 1996), and root growth dynamics associated with soil wetting and drying cycles (Joslin *et al.*, 2000). Here plant access to water was limited by xylem hydraulic conductance (k_R) (mmol m^{-2} MPa^{-1}) of the absorbing root of each soil-root layer, and roots growing in layers with k_R values closer to their maximum (or saturated) values were assumed to be preferentially allocated C:

$$\left(\frac{d\mathbf{C}_R}{dt}\right)_{jk} = \frac{dC_{Rtot}}{dt} f_k(k_R)_j r_k - C_{RD_{jk}} \qquad \text{Eqn 5(a)}$$

where

$$f_k(k_R)_j = \frac{(k_R/k_{Rsat})_j}{\sum_{j=1}^{m}(k_R/k_{Rsat})_j} \qquad \text{Eqn 5(b)}$$

is relative hydraulic conductance, k_{Rsat} is the maximum xylem hydraulic conductance of the root layer, and $r_k = 0.19 - 0.02$ $(k-1)$, where $\sum_{k=1}^{10} r_k = 1$. The constants, 0.19 and 0.02, yield a linear decline in C allocation with increasing root order. TREES computes unique k_{Rsat} values for each root segment using observed well-watered hydraulic properties (i.e. transpiration, predawn and midday water potentials) for the whole plant (Mackay *et al.*, 2015). Use of r_k means that C is allocated proportionally to each root order such that finer roots cost more C, reflective of their faster turnover rate (Joslin *et al.*, 2006; McCormack *et al.*, 2013; Adams *et al.*, 2013). C_{RD} is root C loss to mortality, computed as follows:

$$C_{RD_{jk}} = f_T\left(T_{R_j}\right)\frac{\mathbf{C}_{R_{jk}}}{\tau_{min}(\beta)^{k-1}},\ T_{R_j} > 5 \qquad \text{Eqn 5(c)}$$

where $f_T(T_{R_j}) = \frac{T_{R_j}-5}{20}$, T_R is root temperature (°C), τ_{min} is minimum root life span, and β is the life span rate increase with each increment in root order. This results in faster turnover in lower root orders compared with higher root orders (Joslin *et al.*, 2006; McCormack *et al.*, 2013; Adams *et al.*, 2013). β could be derived empirically, but it was not available for this study and so we set $\beta = 1.25$, a value comparable to those found empirically (e.g. McCormack *et al.*, 2013). Root mortality was assumed to be zero until root temperature exceeds 5°C (Kitajima *et al.*, 2010), thereafter increasing linearly (McCormack & Guo, 2014) until root temperature reached 25°C (Kitajima *et al.*, 2010). For $\tau_{min} = 0.75$ yr and $T_R = 25°$ the life span for the second-order root is 0.94 yr.

Simulations were run for both juniper and piñon at 30 min time steps from 1 January 2012 to 31 December 2016, using meteorological forcing developed for each treatment (ambient,

drought, heat, drought + heat) as follows. For drought treatments (i.e. drought and drought + heat) we reduced precipitation by 45% of ambient beginning in the middle of 2012 and then by 90% of ambient in year 2016 to match the SUMO field experiment (Fig. S2). For heat treatments (i.e. heat and drought + heat) we increased air temperature from ambient by 4.8°C beginning in the middle of 2012. We used measurements to increase shallow (0–15 cm) soil temperature by an average of 3.2°C. Deep soil (15–65 cm) temperatures were computed with a 30 d moving average of shallow soil temperature. Heated treatment deep soil temperature averaged 1.2°C above ambient. Vapor pressure deficit of the air was adjusted from ambient using the increased air temperature and the standard Clausius–Clapeyron equation.

Most model parameters were either site-specific or species-specific taken from the literature (Table S1). Observations of leaf area, leaf gas exchange and water potentials were aggregated from individual trees, weighted using their respective sapwood areas, in each treatment to yield treatment mean values (see Notes S1 for details on these measurements). Fine root diameters and specific root lengths were taken from Pregitzer *et al.* (2002). Root C was distributed among two shallow soil layers (L_{ax} = 0–5 cm and 5–15 cm, L_{lat} = 300 cm), a deep soil layer (L_{ax} = 15–65 cm depth, L_{lat} = 250 cm), a taproot (L_{ax} = 65–290 cm depth, L_{lat} = 0 cm), and a bedrock layer with steady groundwater availability (L_{ax} = 290–300 cm depth, L_{lat} = 120 cm). The main purpose of the taproot was to define dimorphic root architectures with soil layers that were hydraulically separated from the groundwater source at the bottom of the bedrock layer, as opposed to fibrous root architectures with a continuous distribution of fine roots down to the groundwater. In each layer we initialized root C to achieve a root area : leaf area ratio, $R_{R/L}$, of 2.5 for juniper and 1.7 for piñon, consistent with a strategy of juniper preventing root cavitation by reducing the water uptake rate per unit root area (Sperry *et al.*, 2002; West *et al.*, 2008).

At SUMO, the empirical leaf water potential data for both juniper and piñon showed evidence of cavitation reversal during monsoons in years 2012–2015. On the basis of these observations, we forced TREES to reset the xylem water status in the simulated trees (Mackay *et al.*, 2015) at the times of the apparent cavitation reversals. This occurred during monsoon each year, except for 2016 when there was a weak monsoon (see Table S2). Changes made to leaf and root areas since the last refilling event were accounted for in the computation of maximum hydraulic conductance (Sperry *et al.*, 1998; Mackay *et al.*, 2015).

H1: Bedrock groundwater source acquisition

To test the hypothesis H1 that tree hydraulic status is maintained by taking up bedrock groundwater during dry periods and soil water during wetter periods, we used two alternative root area schemes, one with high root area in the bedrock layer and the other with low bedrock root area (Table 1). For the high bedrock root area scheme, we adjusted the C content of the bedrock layer roots to obtain sufficient root area with bedrock groundwater access to match simulated and measured predawn water potentials (Johnson *et al.*, 2018) in the first year of simulation (2012), with the other 4 yr used as a check on the model. Thus, for the high bedrock root area, 14.4% and 11.1% of the initial root area for juniper and piñon, respectively, were supplied with bedrock groundwater. For simulations with low initial bedrock root area (Table 1), the C from the first five root orders in the 290–300 cm layer was redistributed equally among the first five root orders in the soil layers. Thus for the low bedrock root scheme, only 1% of the total initial root area had access to bedrock groundwater. In both schemes, root areas were allowed to adjust dynamically according to Eqn .

Table 1 Root area (A_R) distributions for the high and low bedrock root area schemes by species at initialization of the simulations.

Species	Root layer	Depth range (cm)	High bedrock A_R (% of root area)	Low bedrock A_R (% of root area)
Juniper	Shallow soil	0–5	12.0	15.9
		5–15	17.6	24.9
	Deep soil	15–65	55.8	58.0
	Tap root	65–290	0.2	0.2
	Bedrock	290–300	14.4	1.0
Piñon	Shallow soil	0–5	12.2	16.0
		5–15	24.3	25.0
	Deep soil	15–65	52.2	57.7
	Tap root	65–290	0.2	0.3
	Bedrock	290–300	11.1	1.0

H2: Rates of root growth

To test hypothesis H2, that fine roots must be maintained to access bedrock groundwater because they cannot grow fast enough under drought and heat stress, we quantified how simulated roots were able to grow in the low initial bedrock root area scheme relative to their ability to affect plant water relations. We also quantified the effects of plant water relations and treatment on root growth rate, noting that root growth occurs in all layers as long as their hydraulic conductance is nonzero, and growth occurs in all root orders. The link between plant water relations and root growth rate is via root C cost per unit increment of root area (Eqn) and depends on parameters d_{min} and l_{rs_1}.

Sensitivity analysis

The test for H2 hinges in part on understanding the sensitivity of computed root growth to d_{min} and l_{rs_1}. The species-specific parameters taken from Pregitzer *et al.* (2002) yield very high root tissue densities, and, in turn, high C costs to grow roots. Yet there is potentially a large variability in C costs with and between taxa (Fig. S1), including taxa from which root parameters might be obtained if species-specific ones, such as those used here from Pregitzer *et al.* (2002), are unavailable. Consequently, to understand how the choice of d_{min} and l_{rs_1} affects simulated fine root growth, and place the simulations for juniper and piñon in a larger context, we computed bin averages of parameters based on diameter extremes as well as taxonomic classes (Table 2) from

Table 2 Fine root parameters for computing root dynamics in TREES are root diameter (d_{min}), specific root length (l_{rs_1}) and life span (τ_{min}), representing the life span of the roots at d_{min}. E(d_{min}) is expected value of the minimum diameter.

Taxomic classification	d_{min} (mm)	l_{rs_1} (m g^{-1} C)	RTD (g C cm^{-3})	n	τ_{min} (yr)
Pinaceae	0.47	32.86	0.022	31	0.89
Cupressaceae	0.68	14.69	0.024	6	1.29
Sclerophyllous	0.44	30.00	0.027	1	0.84
Pinus edulis	0.40	22.00	0.045	1	0.76
Juniperus monosperma	0.39	23.00	0.045	1	0.74
$d_{min} > E(d_{min}) + SD(d_{min})$	0.87	12.26	0.017	28	1.65
$d_{min} < E(d_{min}) - SD(d_{min})$	0.18	87.33	0.056	28	0.34

The parameters are derived by taking the means from taxonomic classes in a database of *c*. 900 entries, which was assembled from the literature for this study. (Note that there is also a published database on fine root traits, FRED (https://roots.ornl.gov/).)
The number (*n*) of samples from the database is shown. Minimum life span was computed as a linear function of RTD, $\tau_{min} = 0.75 \times 0.395/d_{min}$. Root tissue density, RTD = $(d_{min} \times l_{rs_1})^{-1}$ with appropriate unit conversions. The extreme diameter (0.87 and 0.18 mm) classes were computed from all evergreen trees in the database ($n = 180$).

published parameter values for a large range of species (Dataset S1). We chose parameters for the respective families (Pinaceae and Cupressaceae) and a Sclerophyllous group to represent climatic adaptation. Extreme large diameters [$d_{min} > E(d_{min}) + SD(d_{min})$], where E($d_{min}$) is expected value of the minimum diameter, were obtained by selecting all 'evergreen trees' entries that had diameters larger than the mean + 1 SD. The extreme minimum values [$d_{min} < E(d_{min}) - SD(d_{min})$] were the subset of evergreen trees with diameters that were smaller than the mean − 1 SD. We parameterized root life span using literature values from studies using minirhizotrons to examine the lifespan of functional roots. We did not find literature values on survival rates specifically for *Pinus edulis* and *Juniperus monosperma* fine roots, but we found studies that reported short (< 1 yr) and long (> 1 yr) fine root life spans (Joslin *et al.*, 2006; Montagnoli *et al.*, 2012), and studies with *Pinus* species with roots of 0.3–0.4 mm diameter having a life span of about 0.75 yr (Withington *et al.*, 2006; McCormack *et al.*, 2013). We used 0.75 yr life span for our 0.395-mm-diameter first-order roots, noting that shorter or longer times would make it costlier or cheaper, respectively, to grow or maintain fine roots. Root life spans were adjusted linearly with diameter relative to the baseline 0.395. Simulations were run for 5 yr at half-hourly time steps on the ambient treatment.

We also considered the sensitivity of $\boldsymbol{A}_R$ to choice of series used to compute r_k. For example, an alternative series described by the recursive function, $r_k = 0.5 r_{k-1}$, where $r_1 = 0.5$, would allocate 75% of root C increment to the first two root orders, compared with 36% allocated using Eqn 5(a–c). The higher allocation of C to the first two root orders would yield a modest 76% increase in $\boldsymbol{A}_R$ increment compared with that produced with Eqn 5(a–c) when the species-specific d_{min} and l_{rs_1} (Pregitzer *et al.*, 2002) are used. By comparison, using the extreme minimum d_{min} and l_{rs_1} instead of species-specific d_{min} and l_{rs_1} would triple the $\boldsymbol{A}_R$ increment. As $\boldsymbol{A}_R$ was more sensitive to the choice of parameters than to the choice of r_k series, we report sensitivity analysis based solely on the r_k series in Eqn 5(a–c) and parameter sets selected from Table 2.

Results

H1: Bedrock groundwater source acquisition

Modeled trees with high initial bedrock root area closely followed the predawn (Fig. 2) and midday water potentials of experimental trees (Fig. S3). Simulated canopy transpiration (E_C) closely followed the dynamics of E_C from sap flux data collected in 2016 (year 5) (Fig. S4). Predawn water potentials remained above −5 and −3 MPa, respectively, for juniper and piñon, in all treatments. Modeled trees with low initial bedrock root area had larger declines in predawn water potentials, with ambient juniper and piñon predawn water potentials reaching −9.5 and −4.0 MPa, respectively, in the first year of simulation. These lower predawn values were maintained for longer periods in the drought, heat and drought + heat treatments, and the values remained lower for the full 5 yr simulation. With low initial bedrock root area, both species also showed increasing time spent with percentage loss of conductance (PLC) in excess of 60%, a potential threshold for hydraulic failure (Adams *et al.*, 2017), over the 5 yr of simulation when exposed to increasing drying (drought + heat > drought > heat > ambient) (Table 3). Juniper had a notable increase in time spent with PLC > 60% in the low bedrock root area scheme, whereas the total time piñon spent at PLC > 60% was insensitive to the initialization of bedrock root area.

For the high initial bedrock root area schemes, the proportion of E_C supplied by bedrock groundwater ranged, among years, from 5.5% to 19.4% for ambient juniper and from 5.3% to 16.6% for ambient piñon. These numbers increased to 24.1–57.1% for drought + heat juniper and 20.2–52.5% for drought + heat piñon. Both species showed similar patterns in shallow soil and bedrock E_C water source, but during the season when there were large interspecific differences in water uptake source it was because juniper took up more bedrock groundwater and piñon took up more shallow soil water (Fig. 3). Alternatively, piñon generally supplied a larger proportion of E_C from shallow soil, especially during the summer/autumn following monsoon. Bedrock groundwater uptake rapidly shifted between near zero immediately after rainfall events and high values during dry periods (Fig. S5). Bedrock groundwater uptake was high during drier periods (e.g. the first 500 d of simulation (Fig. S2)) and low during wetter periods (e.g. in the years 2014 and 2015). Trees initialized with low bedrock root area slowly increased groundwater uptake over time (Fig. 3; compare 2016 with 2012, red vs blue lines), although this was slower for drought + heat than for drought.

H2: Rates of root growth

The extreme differences in leaf water potentials between rooting schemes were mediated by year 5 in the ambient and heat treatments, but remained pronounced in the drought and drought + heat treatments (Fig. 2). The slow adjustment in water

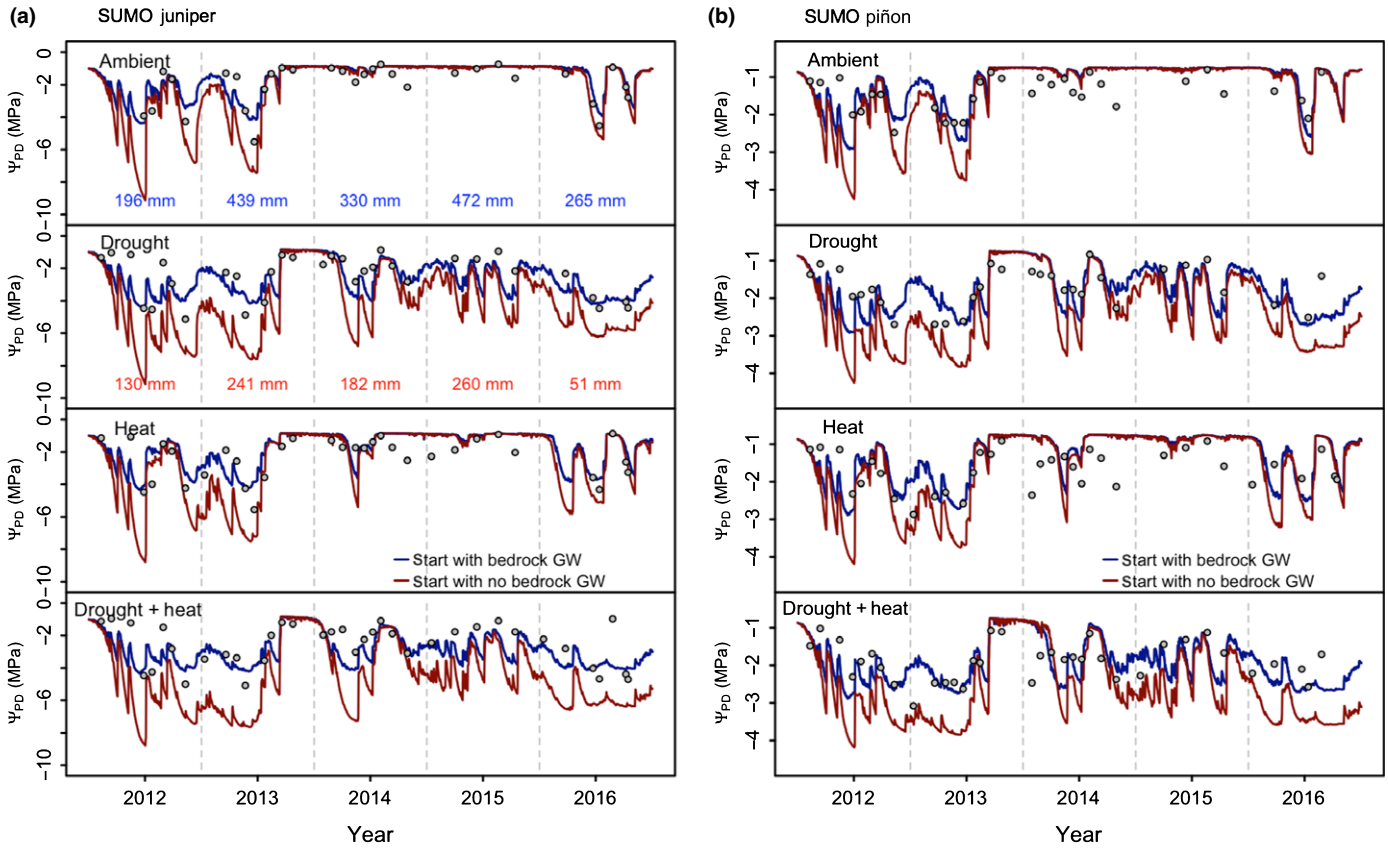

Fig. 2 Simulated predawn water potential (Ψ_{PD}) for juniper (a) and piñon (b) for the 5 yr Los Alamos Survival-Mortality (SUMO) experiment. Plots show simulations with high and low amounts of initial root area within the bedrock layer. Circles are observed predawn water potentials. The numbers in blue, shown within the ambient panels, are ambient annual precipitation amounts, while the numbers in red, shown in the drought panels, are the experimental drought annual precipitation amounts. GW, groundwater.

relations follows a slow rate of change in root : leaf area ratios (Fig. 4). Shallow soil and bedrock layers maintained near steady-state root : leaf area ratios ($R_{R/L}$) when initialized with high bedrock root area in the ambient and drought treatments, and trended downward in heat and heat + drought treatments. Net fine root growth in the first two root orders in the bedrock layer declined with declining leaf predawn water potential, reaching zero net growth at −7.0 MPa for juniper and −3.5 MPa for piñon (Fig. 5). Mean growth rates were reduced by at least 50% in the drought and heat treatments relative to ambient. For the heat + drought treatment, there was negligible net fine root growth, except for juniper at a water potential of −1.0 MPa.

Both species showed lower mean NSC by the year 5 of simulation when exposed to increased drying (drought + heat > drought > heat > ambient) (Table 3). No simulation resulted in exceptionally low NSC, however, with values never deviating outside a range of 3–8% of structural C. Simulations initialized with low bedrock root area had higher NSC amounts than corresponding simulations that were initialized with high bedrock root area.

Sensitivity analysis

Root growth was sensitive to choice of parameter sets for d_{min}, l_{rs_1} and root life span (Fig. 6). For simulations using species-specific parameters, shallow soil and bedrock layers maintained steady-state root areas, while the deep soil layer, which received little infiltrated precipitation, had downward trends in root areas for both species. The use of species-specific parameters resulted in relatively small short-term variability in root areas, and by implication low root growth rates, compared with growth rates obtained using the other parameter sets. At the other extreme, the use of the extremely large diameters [$d_{min} > E(d_{min}) + SD(d_{min})$] parameter set resulted in greater than linear root area growth with time, which led to $R_{R/L}$ values that were doubled relative to those obtained using species-specific parameters, with no appreciable change in transpiration (i.e. 23 mm increase for juniper, and 16 mm increase for piñon over 5 yr).

Discussion

Overarching hypotheses

During dry periods, the SUMO juniper and piñon trees maintained their hydraulic status by taking up water from bedrock sources, as shown by the simulations in this study, with stable isotopes in a previous study at SUMO (Grossiord *et al.*, 2017a), and with piñon and another juniper species in Utah, USA (West *et al.*, 2007a). Hypothesis H1 was supported because simulated trees took up bedrock groundwater when soil layers were dry, but

Table 3 Time spent at percentage loss of conductance (PLC) > 60% over the full 5 yr of simulation (2002–2006), and average nonstructural carbon (NSC) in year 5 of simulation (2016) among species, treatment and initial amount of root area within the bedrock layer.

Species	Initial bedrock root (% of total root area)	Treatment	Time at PLC > 60% (% of 1827 d)	2016 Average NSC (g C m^{-2})
Piñon	11.1	Ambient	36.8	248.3
Piñon	11.1	Drought	80.3	185.5
Piñon	11.1	Heat	49.6	181.3
Piñon	11.1	Drought + heat	94.3	175.0
Piñon	1.0	Ambient	37.0	384.8
Piñon	1.0	Drought	81.0	221.6
Piñon	1.0	Heat	49.0	249.9
Piñon	1.0	Drought + heat	93.2	181.7
Juniper	14.4	Ambient	4.2	280.8
Juniper	14.4	Drought	10.3	189.4
Juniper	14.4	Heat	6.4	188.2
Juniper	14.4	Drought + heat	11.4	179.4
Juniper	1.0	Ambient	14.1	413.1
Juniper	1.0	Drought	42.3	210.4
Juniper	1.0	Heat	22.8	254.9
Juniper	1.0	Drought + heat	56.7	186.4

The NSC values range from 8% of biomass in the simulations of ambient treatments to 3% in the drought + heat treatments. By comparison, observations of NSC at the Los Alamos Survival-Mortality (SUMO) in June 2013 showed ambient values of 10.9% (piñon) and 4.6% (juniper), with values falling to 5.4% (piñon) and remaining unchanged (juniper) in drought + heat treatments (Adams *et al*., 2015; Supporting information Tables S4, S5). These relative differences remained throughout 2016 with generally no decline in NSC (McDowell *et al*., 2019).

switched to soil water uptake following rain events. Hypothesis H2 was also supported because the rates of fine root growth were slow relative to the rate of demand of bedrock groundwater needed to prevent potentially lethal xylem water potentials. Our results imply that these trees must grow into bedrock water sources before drought in order to survive extreme conditions.

H1: Bedrock groundwater source acquisition

During the driest periods, a small fraction of total root area allocated to the bedrock supplied > 60% of transpiration for all treatments, whereas during wetter periods (e.g. ambient treatment, second half of 2013–2015) trees took up negligible bedrock groundwater (Figs 3, S5). Under drought and drought + heat treatments, juniper increased water uptake from bedrock groundwater relative to piñon, particularly during winter and spring, whereas under heat and drought + heat treatments, piñon responded by increasing water uptake from shallow soils during and after monsoons more than was the case for juniper. This is consistent with experimental observations for both species at SUMO using isotopes of water (Grossiord *et al*., 2017a) and for piñon in other studies (West *et al*., 2007a,b). Juniper was more anisohydric (i.e. had more daily variation in water potential; Tardieu & Simonneau, 1998) than piñon, dried out the shallow soil layers, and thus depended on more deeply infiltrating winter rainfall as well as bedrock groundwater, as has been shown previously (Plaut *et al*., 2013; Grossiord *et al*., 2017a). These contrasting trait responses follow directly from the species' contrasting xylem cavitation vulnerability curves (Mackay *et al*., 2015; Garcia-Forner *et al*., 2016).

Modeled trees spent an increasing amount of time at PLC > 60% with intensity of treatment (drought + heat > drought > heat > ambient) (Table 3). Piñon had PLC values that potentially predisposed them to drought-induced mortality (Adams *et al*., 2017) despite maintaining relatively high water potentials compared with simulations of warm droughts that did not consider bedrock groundwater (McDowell *et al*., 2016). Alternatively, when bedrock groundwater access was reduced, modeled trees in all treatments experienced potentially lethal predawn water potentials for extensive periods of time (Fig. 2), which were well below thresholds used previously to predict mortality (i.e. April–August mean water potentials of −5.3 MPa for juniper and −2.4 MPa for piñon; McDowell *et al*., 2016). Juniper responded to an impaired bedrock groundwater with a notable increase in time spent at high PLC, whereas piñon showed no such response. This follows from piñon's greater ability to respond to small rainfall events that penetrate only shallow soil water layers at SUMO (Grossiord *et al*., 2017a) and other locations (West *et al*., 2007a,b; Plaut *et al*., 2013).

H2: Rates of root growth

Root area : leaf area ratio, $R_{R/L}$, adjusted slowly (Fig. 4) because of slow root growth (Fig. 5), requiring seasons to years to change water-uptake rates. The slow root growth was not attributed to a lack of C resources, as the biggest decline in NSC was 26% relative to the least-stressed treatment (i.e. ambient initialized with high root area in the bedrock) (Table 3). This was well below a lethal decline (Anderegg & Anderegg, 2013; Adams *et al*., 2017). Simulations initialized with low bedrock root area maintained relatively higher NSC because the allocation of C to growth declined more rapidly than photosynthesis when PLC was > 50% (Mackay *et al*., 2015).

We considered the possibility that the slow root growth was an artifact of either model parameterization or an overly conservative algorithm for determining the allocation of NSC to growth. Two lines of evidence suggest there were no such artifacts. First, parameters that favored the highest growth rates would not have allowed root area to increase enough to mediate the effects of drought during the relative dry first 500 d of simulation. Second, the parameter set that was most favorable for high root growth rates would have more than doubled $R_{R/L}$ by the year 5 of simulation (Fig. 6), which most certainly would have overbuilt the root areas for piñon and juniper (West *et al*., 2008), resulting in suboptimal water transport (Sperry *et al*., 2002). No matter what root trait parameter values were used, the fine root growth would not do the job of maintaining tree hydraulic status after the onset of drought. Moreover, a more aggressive use of NSC for growth allocation that did not overbuild roots would have increased leaf area, contrary to observations in the experimental treatments

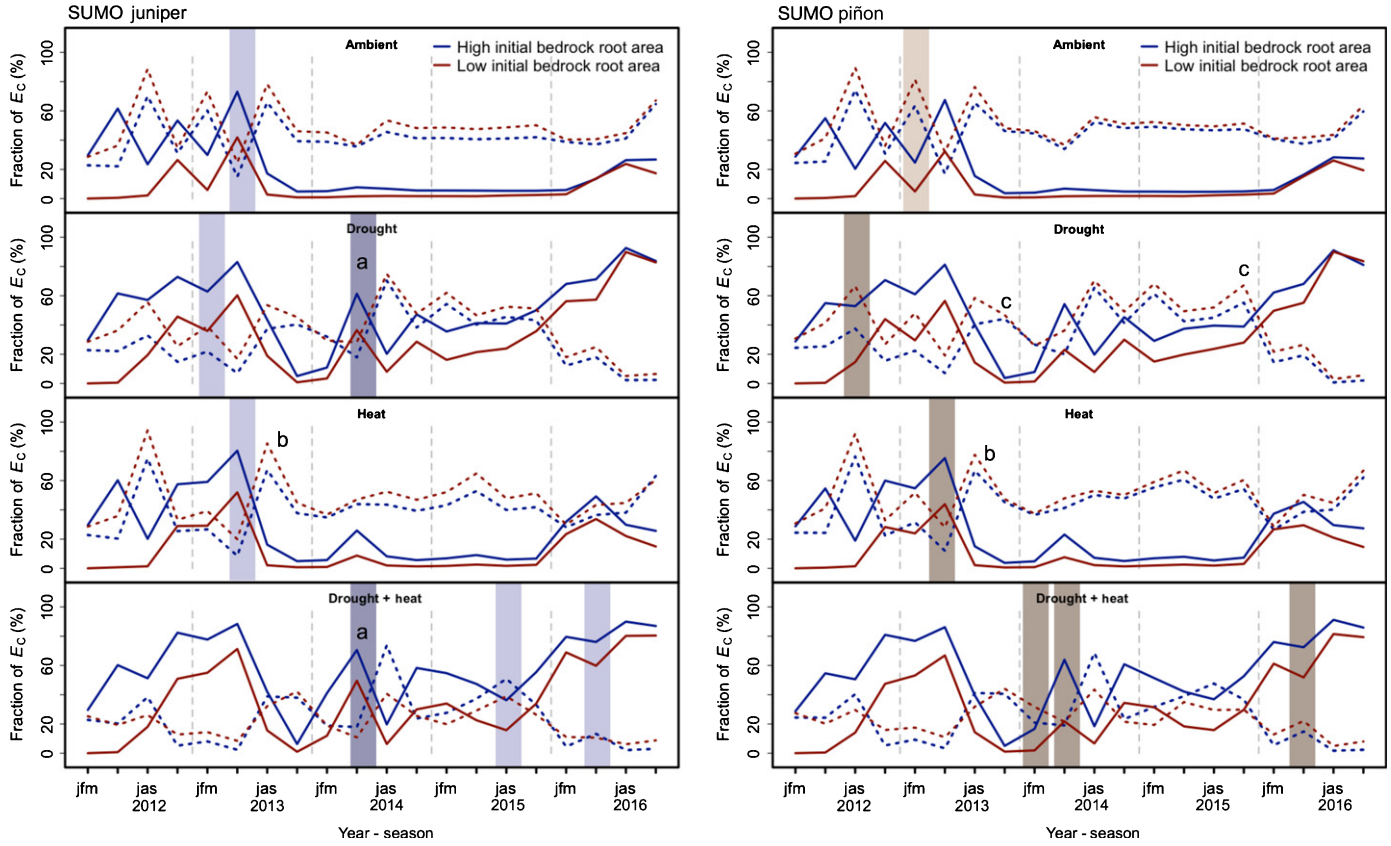

Fig. 3 Relative contributions of bedrock and shallow soil to canopy transpiration, E_C. Simulations are aggregated to 3 month groups (jfm, January, February, March; jas, July, August, September). Blue and red lines represent high and low initial bedrock root area simulations, respectively. Solid lines are bedrock water uptake and dashed lines are shallow soil water uptake. Darker blue shaded boxes indicate where groundwater uptake by one species exceeded that by the other species by > 10% of E_C, based on the fluxes from the low initial bedrock root area simulations. Darker brown shaded boxes indicate where shallow soil water uptake by one species exceeded the other species by > 10% of E_C, also for the simulations initialized with low bedrock root area. The lighter shaded boxes indicate where the respective fluxes differ by > 8% but < 10% of E_C. All differences ≤ 8% of E_C are not highlighted. The labels a–c are used to highlight periods where significant differences in water uptake reported by Grossiord *et al*. (2017a) using water isotopes are reproduced by these simulations. Specifically, 'a' shows relatively higher bedrock water uptake by juniper in the drought treatments during a normal year (i.e. 2014); 'b' shows juniper increasing its uptake of shallow soil in the heat treatment compared with ambient treatment, while piñon does not (i.e. small difference between red and blue dashed lines); and 'c' shows that piñon uses more shallow water during the fall recover period in wet years (i.e. 2015) compared with dry years (i.e. 2013).

(Adams *et al*., 2015; McBranch *et al*., 2018; McDowell *et al*., 2019).

The results here also lend mechanistic support to explain tree recovery post-drought. Prolonged drought inhibits the ability of trees to recover when drought is relieved, and this has been attributed to a lack of C sequestered during drought or to declining C reserves (Trugman *et al*., 2018). The simulations here add an additional explanation for the observed survival or mortality of piñon-juniper woodlands, in particular, and woody systems in general, which is that fine root growth is too slow to allow for rapid tree hydraulic recovery after drought even if drought does not cause a substantial decline in C reserves. Use of existing roots with access to reliable water during drought obviates the need for rapid root growth, and offers an explanation for the rapid shifts seen in water-uptake sources during drought and rapid return to shallower layers following precipitation events (Dawson, 1993; Burgess *et al*., 1998; Joslin *et al*., 2000; Barton & Montagu, 2006; Metcalfe *et al*., 2008; Bleby *et al*., 2010). The simulations here presume that such rapid changes are passive responses to pressure gradients. The underlying mechanisms are likely to be more complex, such as an active control over root water uptake via refilling of shallow-rooted piñon roots (West *et al*., 2007a) or expression of aquaporins (Gambetta *et al*., 2012; Venturas *et al*., 2017). Rapid fine root growth (Barnes, 2002; Laclau *et al*., 2013) may be restricted to more productive systems than piñon-juniper woodlands, in actively developing plants that may be more able to alter their $R_{R/L}$ than mature individuals.

Broader implications

As we gain an improved understanding of abiotic controls over the heterogeneity of reliable water sources to support tree survival under climate change-type droughts (McLaughlin *et al*., 2017), there is a need for a complementary understanding of the physiological responses to these water sources. The model presented here addresses a significant knowledge gap in understanding such

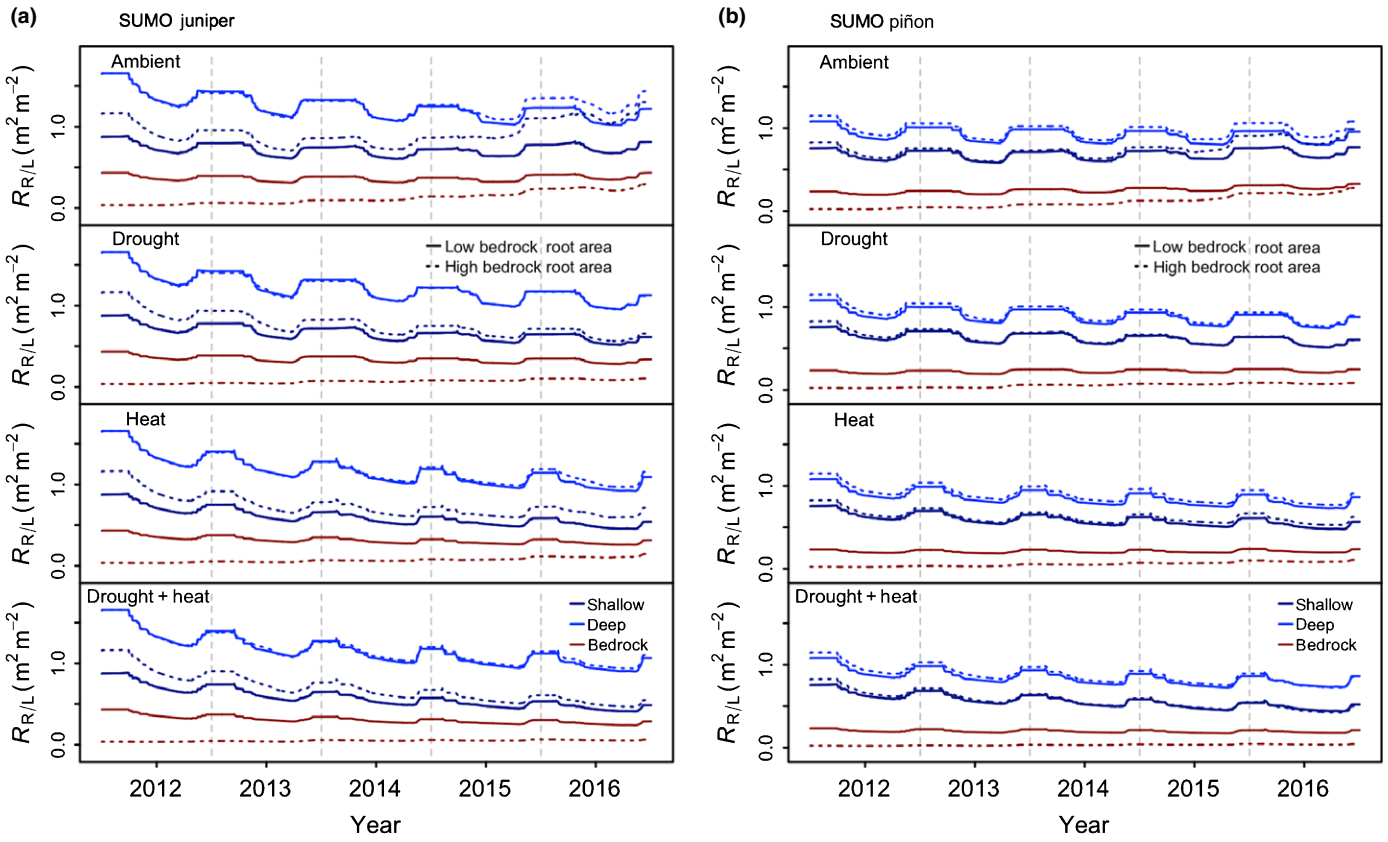

Fig. 4 Simulated root : leaf area ratios ($R_{R/L}$) for juniper (a) and piñon (b), initializing TREES with high (14.4% for juniper, 11.1% for piñon) and low (1% for both species) percentage of the root area with access to bedrock groundwater. The seasonal cycle is dominated by the change in leaf area associated with leaf phenology. Total $R_{R/L}$ by plot can be computed by summing shallow, deep, and bedrock values at a given point in time.

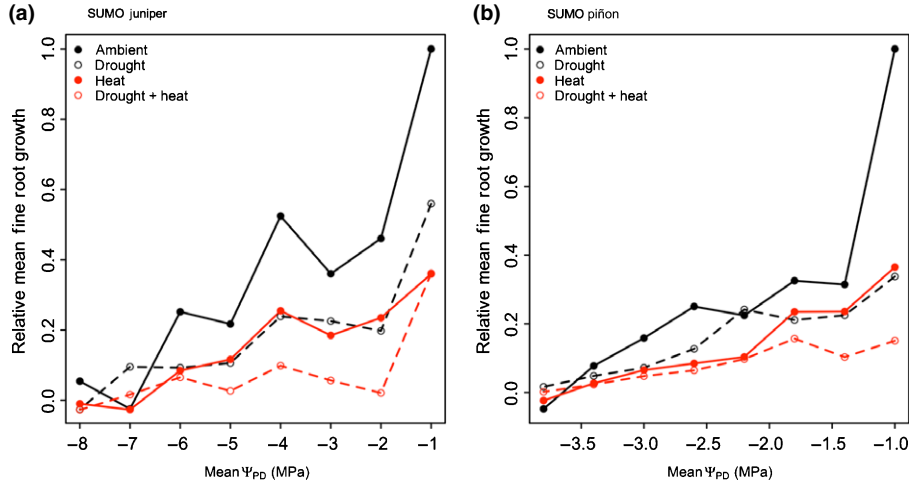

Fig. 5 Simulated relative rate of growth of juniper (a) and piñon (b) first- and second-order roots (summed) in the bedrock layer as a function of mean predawn water potential. Results are for simulations that were initialized with 1% of fine roots in the bedrock and then roots were allowed to grow. Open circles and dashed lines had reduced precipitation, and red circles represented heat treatment. Growth was computed as the difference in sum of first- and second-order root carbon content between consecutive days. The mean of these results was then computed for each bin of predawn water potential, with steps of 0.4 and 1.0 MPa for piñon and juniper, respectively.

biotic–abiotic processes because it explicitly links C allocation and plant hydraulics (Fisher *et al.*, 2018; Hartmann *et al.*, 2018). This model was used to explain why trees frequently maintain deep coarse root systems with only small amounts of absorbing fine roots (Laclau *et al.*, 2013; Pinheiro *et al.*, 2016) to obtain a high proportion of water from deeper groundwater sources during drought (David *et al.*, 2007; Miller *et al.*, 2010; Grossiord *et al.*, 2017a). The simulations also provide a mechanistic

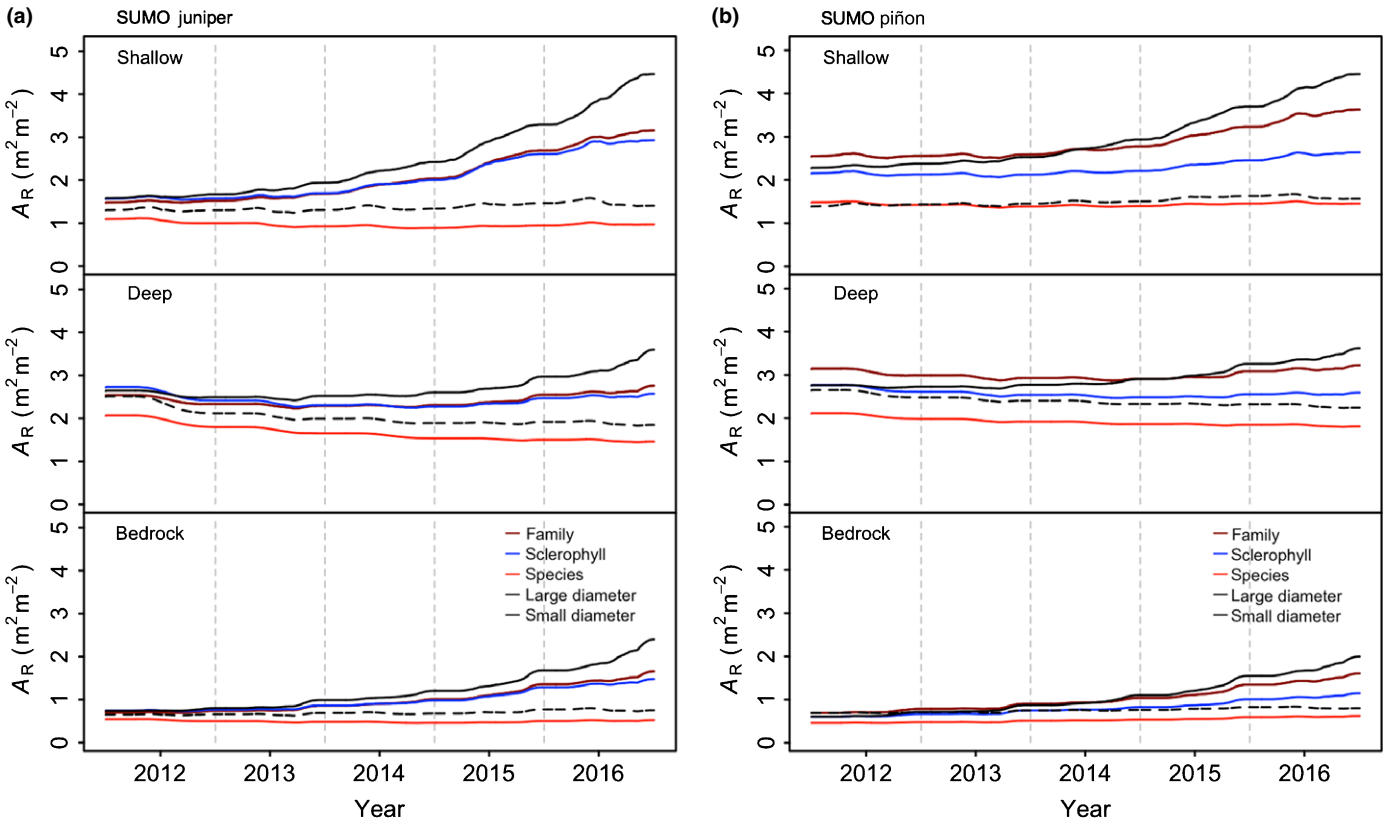

Fig. 6 Variability of juniper (a) and piñon (b) root growth in shallow soil, deep soil and bedrock layers in response to differences in root diameter, specific root length and minimum root lifespan parameters. The 'family' simulations used aggregate parameters for the respective families for the species; 'sclerophyll' represents dry-adapted woody species; 'species' represents the respective species-level observations; and 'large diameter' and 'small diameter' aggregate the parameters by taking the cluster of data from above and below the mean +1 SD or mean − 1 SD, respectively, of the root diameters. Roots are grown using the Los Alamos Survival-Mortality (SUMO) ambient plot conditions over 5 yr.

explanation for the lack of fine root growth seen during drought (Joslin *et al.*, 2000; Metcalfe *et al.*, 2008), and supports the observation that trees make sufficient C investments in fine roots before drought, enabling them to gain access to reliable water for survival during drought (Jackson *et al.*, 1999; Rose *et al.*, 2003; Eberbach & Burrows, 2006; Johnson *et al.*, 2018). The new modeling approach could be adapted for use with other hydraulically sensitive ecosystem models, and tested in a wide range of systems, including where roots do not have access to reliable water sources. The modified Trees model demonstrates how fine root growth could be integrated into ecosystem models (McCormack *et al.*, 2015) and answers a broader call for constraining ecosystem models with observations (Law, 2014).

Acknowledgements

This work was funded by the National Science Foundation IOS-1450679 to DSM and IOS-1450650 to JSS. DSM acknowledges additional support from NSF IOS-1444571 and IOS-1547796. NGM relied on support from Pacific Northwest National Lab's LDRD program. CG was supported by the Swiss National Science Foundation SNF (5231.00639.001.01). The contents of this manuscript reflect the views of the authors and do not necessarily reflect the views of the aforementioned funding agencies. Three anonymous reviewers are thanked for comments that improved the manuscript. Trees model code and input files for this study are available at https://github.com/dscottmackay/root_growth_TREES_paper.

Author contributions

DSM led the model theory development, developed the model, and wrote the manuscript; PRS assisted with the model theory development and edited the manuscript; JRP, XT and DRW assisted with the model development and edited the manuscript; CG, HDA and NGM designed the field experiment, conducted fieldwork and edited the manuscript; JSS helped with conceptual design of the model and edited the manuscript.

ORCID

Henry D. Adams https://orcid.org/0000-0001-9630-4305
Charlotte Grossiord https://orcid.org/0000-0002-9113-3671
D. Scott Mackay https://orcid.org/0000-0003-0477-9755
Nathan G. McDowell https://orcid.org/0000-0002-2178-2254
John S. Sperry https://orcid.org/0000-0001-7881-7393
Diane R. Wang https://orcid.org/0000-0002-2290-3257

References

Aaltonen H, Lindén A, Heinonsalo J, Biasi C, Pumpanen J. 2016. Effects of prolonged drought stress on Scots pine seedling carbon allocation. *Tree Physiology* **37**: 418–437.

Adams HD, Collins AD, Briggs SP, Vennetier M, Dickman LT, Sevanto SA, Garcia-Forner N, Powers HH, Mcdowell NG. 2015. Experimental drought and heat can delay phenological development and reduce foliar and shoot growth in semiarid trees. *Global Change Biology* **21**: 4210–4220.

Adams HD, Guardiola-Claramonte M, Barron-Gafford GA, Villegas JC, Breshears DD, Zou CB, Troch PA, Huxman TE. 2009. Temperature sensitivity of drought-induced tree mortality portends increased regional die-off under global-change-type drought. *Proceedings of the National Academy of Sciences, USA* **106**: 7063–7066.

Adams HD, Zeppel MJB, Anderegg WRL, Hartmann H, Landhäusser SM, Tissue DT, Huxman TE, Hudson PJ, Franz TE, Allen CD *et al.* 2017. A multi-species synthesis of physiological mechanisms in drought-induced tree mortality. *Nature Ecology & Evolution* **1**: 1–7.

Adams TS, McCormack ML, Eissenstat DM. 2013. Foraging strategies in trees of different root morphology: the role of root lifespan. *Tree Physiology* **33**: 940–948.

Anderegg WRL. 2012. Complex aspen forest carbon and root dynamics during drought. *Climatic Change* **111**: 983–991.

Anderegg WRL, Anderegg LDL. 2013. Hydraulic and carbohydrate changes in experimental drought-induced mortality of saplings in two conifer species. *Tree Physiology* **33**: 252–260.

Barbeta A, Mejía-Chang M, Ogaya R, Voltas J, Dawson TE, Penuelas J. 2015. The combined effects of a long-term experimental drought and an extreme drought on the use of plant-water sources in a Mediterranean forest. *Global Change Biology* **21**: 1213–1225.

Barnes AD. 2002. Effects of phenology, water availability and seed source on loblolly pine biomass partitioning and transpiration. *Tree Physiology* **22**: 733–740.

Barton CVM, Montagu KD. 2006. Effect of spacing and water availability on root:shoot ratio in Eucalyptus camaldulensis. *Forest Ecology and Management* **221**: 52–62.

Bauhus J, Messier C. 1999. Soil exploitation strategies of fine roots in different tree species of the southern boreal forest of eastern Canada. *Canadian Journal of Forest Research* **29**: 260–273.

Bleby TM, McElrone AJ, Jackson RB. 2010. Water uptake and hydraulic redistribution across large woody root systems to 20 m depth. *Plant, Cell & Environment* **33**: 2132–2148.

Bowsher AW, Mason CM, Goolsby EW, Donovan LA. 2016. Fine root tradeoffs between nitrogen concentration and xylem vessel traits preclude unified whole-plant resource strategies in *Helianthus*. *Ecology and Evolution* **6**: 1016–1031.

Burgess S, Adams M, Turner N, Ong C. 1998. The redistribution of soil water by tree root systems. *Oecologia* **115**: 306–311.

Chen W, Zeng H, Eissenstat DM, Guo D. 2013. Variation of first-order root traits across climatic gradients and evolutionary trends in geological time. *Global Ecology and Biogeography* **22**: 846–856.

Cheng L, Chen W, Adams TS, Wei X, Li L, McCormack ML, DeForest JL, Koide RT, Eissenstat DM. 2016. Mycorrhizal fungi and roots are complementary in foraging within nutrient patches. *Ecology* **97**: 2815–2823.

Comas LH, Becker SR, Cruz VMV, Byrne PF, Dierig DA. 2013. Root traits contributing to plant productivity under drought. *Frontiers in Plant Science* **4**: 442. doi: 10.3389/fpls.2013.00442.

Comas LH, Bouma T, Eissenstat DM. 2002. Linking root traits to potential growth rate in six temperate tree species. *Oecologia* **132**: 34–43.

Comas LH, Callahan HS, Midford PE. 2014. Patterns in root traits of woody species hosting arbuscular and ectomycorrhizas: implications for the evolution of belowground strategies. *Ecology and Evolution* **4**: 2979–2990.

Comas LH, Eissenstat DM. 2009. Patterns in root trait variation among 25 co-existing North American forest species. *New Phytologist* **182**: 919–928.

Cuneo IF, Knipfer T, Brodersen CR, Mcelrone AJ. 2016. Mechanical failure of fine root cortical cells initiates plant hydraulic decline during drought. *Plant Physiology* **172**: 1669–1678.

David TS, Henriques MO, Kurz-Besson C, Nunes J, Valente F, Vaz M, Pereira JS, Siegwolf R, Chaves MM, Gazarini LC *et al.* 2007. Water-use strategies in two co-occurring Mediterranean evergreen oaks: surviving the summer drought. *Tree Physiology* **27**: 793–803.

Dawson TE. 1993. Hydraulic lift and water-use by plants – implications for water-balance, performance and plant-plant interactions. *Oecologia* **95**: 565–574.

Doughty CE, Malhi Y, Araujo-Murakami A, Metcalfe DB, Silva-Espejo JE, Arroyo L, Heredia JP, Pardo-Toledo E, Mendizabal LM, Rojas-Landivar VD *et al.* 2014. Allocation trade-offs dominate the response of tropical forest growth to seasonal and interannual drought. *Ecology* **95**: 2192–2201.

Eberbach PL, Burrows GE. 2006. The transpiration response by four topographically distributed Eucalyptus species, to rainfall occurring during drought in south eastern Australia. *Physiologia Plantarum* **127**: 483–493.

Eissenstat DM, Kucharski JM, Zadworny M, Adams TS, Koide RT. 2015. Linking root traits to nutrient foraging in arbuscular mycorrhizal trees in a temperate forest. *New Phytologist* **208**: 114–124.

Ewers B, Oren R, Sperry J. 2000. Influence of nutrient versus water supply on hydraulic architecture and water balance in *Pinus taeda*. *Plant, Cell & Environment* **23**: 1055–1066.

Fan Y, Miguez-Macho G, Jobbágy EG, Jackson RB, Otero-Casal C. 2017. Hydrologic regulation of plant rooting depth. *Proceedings of the National Academy of Sciences, USA* **114**: 10572–10577.

Fisher RA, Koven CD, Anderegg WRL, Christoffersen BO, Dietze MC, Farrior CE, Holm JA, Hurtt GC, Knox RG, Lawrence PJ *et al.* 2018. Vegetation demographics in Earth System Models: a review of progress and priorities. *Global Change Biology* **24**: 35–54.

Gambetta GA, Manuck CM, Drucker ST, Shaghasi T, Fort K, Matthews MA, Walker MA, McElrone AJ. 2012. The relationship between root hydraulics and scion vigour across *Vitis* rootstocks: what role do root aquaporins play? *Journal of Experimental Botany* **63**: 6445–6455.

Garcia-Forner N, Adams HD, Sevanto S, Collins AD, Dickman LT, Hudson PJ, Zeppel MJB, Jenkins MW, Powers H, Martínez-Vilalta J *et al.* 2016. Responses of two semiarid conifer tree species to reduced precipitation and warming reveal new perspectives for stomatal regulation. *Plant, Cell & Environment* **39**: 38–49.

Gholz H. 1982. Environmental limits on aboveground net primary production, leaf area, and biomass in vegetation zones of the Pacific Northwest. *Ecology* **63**: 469–481.

Gower ST, Vogt KA, Grier CC. 1992. Carbon dynamics of rocky-mountain Douglas-fir – influence of water and nutrient availability. *Ecological Monographs* **62**: 43–65.

Grier C, Running S. 1977. Leaf area of mature northwestern coniferous forests: relation to site water balance. *Ecology* **58**: 893–899.

Grossiord C, Sevanto S, Borrego I, Chan AM, Collins AD, Dickman LT, Hudson PJ, McBranch N, Michaletz ST, Pockman WT *et al.* 2017b. Tree water dynamics in a drying and warming world. *Plant, Cell & Environment* **40**: 1861–1873.

Grossiord C, Sevanto S, Dawson TE, Adams HD, Collins AD, Dickman LT, Newman BD, Stockton EA, McDowell NG. 2017a. Warming combined with more extreme precipitation regimes modifies the water sources used by trees. *New Phytologist* **213**: 584–596.

Hacke UG, Sperry JS, Ewers BE, Ellsworth DS, Schafer KVR, Oren R. 2000. Influence of soil porosity on water use in *Pinus taeda*. *Oecologia* **124**: 495–505.

Hartmann H. 2011. Will a 385 million year-struggle for light become a struggle for water and for carbon? – How trees may cope with more frequent climate change-type drought events. *Global Change Biology* **17**: 642–655.

Hartmann H, Moura CF, Anderegg WRL, Ruehr NK, Salmon Y, Allen CD, Arndt SK, Breshears DD, Davi H, Galbraith D *et al.* 2018. Research frontiers for improving our understanding of drought-induced tree and forest mortality. *New Phytologist* **218**: 15–28.

Hendrick RL, Pregitzer KS. 1996. Temporal and depth-related patterns of fine root dynamics in northern hardwood forests. *Journal of Ecology* **84**: 167–176.

Hertel D, Strecker T, Müller-Haubold H, Leuschner C. 2013. Fine root biomass and dynamics in beech forests across a precipitation gradient – is optimal resource partitioning theory applicable to water-limited mature trees? *Journal of Ecology* **101**: 1183–1200.

Jackson RB, Moore LA, Hoffmann WA, Pockman WT, Linder CR. 1999. Ecosystem rooting depth determined with caves and DNA. *Proceedings of the National Academy of Sciences, USA* **96**: 11387–11392.

Johnson DM, Domec J-C, Carter Berry Z, Schwantes AM, Mcculloh KA, Woodruff DR, Wayne Polley H, Wortemann R, Swenson JJ, Scott Mackay D *et al.* 2018. Co-occurring woody species have diverse hydraulic strategies and mortality rates during an extreme drought. *Plant, Cell & Environment* **41**: 576–588.

Johnson NC, Angelard C, Sanders IR, Kiers ET. 2013. Predicting community and ecosystem outcomes of mycorrhizal responses to global change. *Ecology Letters* **16**: 140–153.

Joslin JD, Gaudinski JB, Torn MS, Riley WJ, Hanson PJ. 2006. Fine-root turnover patterns and their relationship to root diameter and soil depth in a ^{14}C-labeled hardwood forest. *New Phytologist* **172**: 523–535.

Joslin JD, Wolfe MH, Hanson PJ. 2000. Effects of altered water regimes on forest root systems. *New Phytologist* **147**: 117–129.

Kitajima K, Anderson KE, Allen MF. 2010. Effect of soil temperature and soil water content on fine root turnover rate in a California mixed conifer ecosystem. *Journal of Geophysical Research* **115**.

Kozlowski TT, Pallardy SG. 2002. Acclimation and adaptive responses of woody plants to environmental stresses. *Botanical Review* **68**: 270–334.

Kramer-Walter KR, Bellingham PJ, Millar TR, Smissen RD, Richardson SJ, Laughlin DC. 2016. Root traits are multidimensional: specific root length is independent from root tissue density and the plant economic spectrum. *Journal of Ecology* **104**: 1299–1310.

Laclau J-P, Da Silva EA, Lambais GR, Bernoux M, Le Maire G, Stape JL, Bouillet J-P, de Moraes Gonçalves JL, Jourdan C, Nouvellon Y. 2013. Dynamics of soil exploration by fine roots down to a depth of 10 m throughout the entire rotation in *Eucalyptus grandis* plantations. *Frontiers in Plant Science* **4**: 243.

Law BE. 2014. Regional analysis of drought and heat impacts on forests: current and future science directions. *Global Change Biology* **20**: 3595–3599.

Li FL, Bao WK. 2015. New insights into leaf and fine-root trait relationships: implications of resource acquisition among 23 xerophytic woody species. *Ecology and Evolution* **5**: 5344–5351.

Liu Y, Li P, Wang G, Liu G, Li Z. 2016. Above- and below-ground biomass distribution and morphological characteristics respond to nitrogen addition in *Pinus tabuliformis*. *New Zealand Journal of Forestry Science* **46**: 1–9.

Ma Z, Guo D, Xu X, Lu M, Bardgett RD, Eissenstat DM, McCormack ML, Hedin LO. 2018. Evolutionary history resolves global organization of root functional traits. *Nature* **555**: 1–20.

Mackay DS, Roberts DE, Ewers BE, Sperry JS, McDowell NG, Pockman WT. 2015. Interdependence of chronic hydraulic dysfunction and canopy processes can improve integrated models of tree response to drought. *Water Resources Research* **51**: 6156–6176.

Magnani F, Grace J, Borghetti M. 2002. Adjustment of tree structure in response to the environment under hydraulic constraints. *Functional Ecology* **16**: 385–393.

Makita N, Kosugi Y, Dannoura M, Takanashi S, Niiyama K, Kassim AR, Nik AR. 2012. Patterns of root respiration rates and morphological traits in 13 tree species in a tropical forest. *Tree Physiology* **32**: 303–312.

McBranch NA, Grossiord C, Adams H, Borrego I, Collins AD, Dickman T, Ryan M, Sevanto S, McDowell NG. 2018. Lack of acclimation of leaf area: sapwood area ratios in piñon pine and juniper in response to precipitation reduction and warming. *Tree Physiology* **21**: 4210–4218.

McCormack ML, Adams TS, Smithwick EAH, Eissenstat DM. 2013. Predicting fine root lifespan from plant functional traits in temperate trees. *New Phytologist* **195**: 823–831.

McCormack ML, Dickie IA, Eissenstat DM, Fahey TJ, Fernandez CW, Guo D, Helmisaari H-S, Hobbie EA, Iversen CM, Jackson RB *et al.* 2015. Redefining fine roots improves understanding of below-ground contributions to terrestrial biosphere processes. *New Phytologist* **207**: 505–518.

McCormack ML, Guo D. 2014. Impacts of environmental factors on fine root lifespan. *Frontiers in Plant Science* **5**: 205.

McDowell NG, Grossiord C, Adams HD, Pinzón-Navarro S, Mackay DS, Breshears DD, Allen CD, Borrego I, Dickman LT, Collins A *et al.* 2019. Mechanisms of a coniferous woodland persistence under drought and heat. *Environmental Research Letters* **14**: 045014.

McDowell NG, Williams AP, Xu C, Pockman WT, Dickman LT, Sevanto S, Pangle R, Limousin J, Plaut J, Mackay DS *et al.* 2016. Multi-scale predictions of massive conifer mortality due to chronic temperature rise. *Nature Climate Change* **6**: 295–300.

McLaughlin BC, Ackerly DD, Klos PZ, Natali J, Dawson TE, Thompson SE. 2017. Hydrologic refugia, plants, and climate change. *Global Change Biology* **23**: 2941–2961.

Meier IC, Leuschner C. 2008. Belowground drought response of European beech: fine root biomass and carbon partitioning in 14 mature stands across a precipitation gradient. *Global Change Biology* **14**: 2081–2095.

Mencuccini M, Minunno F, Salmon Y, Martínez-Vilalta J, Holtta T. 2015. Coordination of physiological traits involved in drought-induced mortality of woody plants. *New Phytologist* **208**: 396–409.

Metcalfe DB, Meir P, Aragão LEOC, da Costa ACL, Braga AP, Gonçalves PHL, de Athaydes Silva Junior J, de Almeida SS, Dawson LA, Malhi Y *et al.* 2008. The effects of water availability on root growth and morphology in an Amazon rainforest. *Plant and Soil* **311**: 189–199.

Miller GR, Chen X, Rubin Y, Ma S, Baldocchi DD. 2010. Groundwater uptake by woody vegetation in a semiarid oak savanna. *Water Resources Research* **46**: 273–214.

Montagnoli A, Terzaghi M, Di Iorio A, Scippa GS, Chiatante D. 2012. Fine-root morphological and growth traits in a Turkey-oak stand in relation to seasonal changes in soil moisture in the Southern Apennines, Italy. *Ecological Research* **27**: 1015–1025.

Moser G, Schuldt B, Hertel D, Horna V, Coners H, Barus H, Leuschner C. 2014. Replicated throughfall exclusion experiment in an Indonesian perhumid rainforest: wood production, litter fall and fine root growth under simulated drought. *Global Change Biology* **20**: 1481–1497.

Newman BD, Campbell AR, Norman DI, Ringelberg DB. 1997. A model for microbially induced precipitation of vadose-zone calcites in fractures at Los Alamos, New Mexico, USA. *Geochimica Et Cosmochimica Acta* **61**: 1783–1792.

Ostonen I, Püttsepp Ü, Biel C, Alberton O, Bakker MR, Löhmus K, Majdi H, Metcalfe D, Olsthoorn AFM, Pronk A *et al.* 2007. Specific root length as an indicator of environmental change. *Plant Biosystems* **141**: 426–442.

Padilla FM, Pugnaire FI. 2007. Rooting depth and soil moisture control Mediterranean woody seedling survival during drought. *Functional Ecology* **21**: 489–495.

Pinheiro RC, de Deus JC Jr, Nouvellon Y, Campoe OC, Stape JL, Aló LL, Guerrini IA, Jourdan C, Laclau J-P. 2016. A fast exploration of very deep soil layers by Eucalyptus seedlings and clones in Brazil. *Forest Ecology and Management* **366**: 143–152.

Pittermann J, Stuart SA, Dawson TE, Moreau A. 2012. Cenozoic climate change shaped the evolutionary ecophysiology of the Cupressaceae conifers. *Proceedings of the National Academy of Sciences, USA* **109**: 9647–9652.

Plaut JA, Wadsworth WD, Pangle R, Yepez EA, Mcdowell NG, Pockman WT. 2013. Reduced transpiration response to precipitation pulses precedes mortality in a piñon–juniper woodland subject to prolonged drought. *New Phytologist* **200**: 375–387.

Pregitzer KS, DeForest JL, Burton AJ, Allen MF, Ruess RW, Hendrick RL. 2002. Fine root architecture of nine North American trees. *Ecological Monographs* **72**: 293–309.

Pregitzer K, Laskowski M, Burton A, Lessard V, Zak D. 1998. Variation in sugar maple root respiration with root diameter and soil depth. *Tree Physiology* **18**: 665–670.

Reich PB, Tjoelker MG, Walters MB, Vanderklein DW, Buschena C. 1998. Close association of RGR, leaf and root morphology, seed mass and shade tolerance in seedlings of nine boreal tree species grown in high and low light. *Functional Ecology* **12**: 327–338.

Rose K, Graham R, Parker D. 2003. Water source utilization by *Pinus jeffreyi* and *Arctostaphylos patula* on thin soils over bedrock. *Oecologia* **134**: 46–54.

Ruehr NK, Offermann CA, Gessler A, Winkler JB, Ferrio JP, Buchmann N, Barnard RL. 2009. Drought effects on allocation of recent carbon: from beech leaves to soil CO_2 efflux. *New Phytologist* **184**: 950–961.

Savoy P, Mackay DS. 2015. Modeling the seasonal dynamics of leaf area index based on environmental constraints to canopy development. *Agricultural and Forest Meteorology* **200**: 46–56.

Sperry JS, Adler FR, Campbell GS, Comstock JP. 1998. Limitation of plant water use by rhizosphere and xylem conductance: results from a model. *Plant, Cell & Environment* **21**: 347–359.

Sperry JS, Hacke U, Oren R, Comstock J. 2002. Water deficits and hydraulic limits to leaf water supply. *Plant, Cell & Environment* **25**: 251–263.

Sperry JS, Wang Y, Wolfe BT, Mackay DS, Anderegg WRL, Mcdowell NG, Pockman WT. 2016. Pragmatic hydraulic theory predicts stomatal responses to climatic water deficits. *New Phytologist* **212**: 577–589.

Tai X, Mackay DS, Anderegg WRL, Sperry JS, Brooks PD. 2017. Plant hydraulics improves and topography mediates prediction of aspen mortality in southwestern USA. *New Phytologist* **213**: 113–127.

Tai X, Mackay DS, Sperry JS, Brooks P, Anderegg WRL, Flanagan LB, Rood SB, Hopkinson C. 2018. Distributed plant hydraulic and hydrological modeling to understand the susceptibility of riparian woodland trees to drought-induced mortality. *Water Resources Research* **54**: 4901–4915.

Tardieu F, Simonneau T. 1998. Variability among species of stomatal control under fluctuating soil water status and evaporative demand: modelling isohydric and anisohydric behaviours. *Journal of Experimental Botany* **49**: 419–432.

Teskey RO, Hinckley TM. 1981. Influence of temperature and water potential on root growth of white oak. *Physiologia Plantarum* **52**: 363–369.

Tierney GD, Foxx TS. 1982. *Floristic composition and plant succession on near-surface radioactive-waste-disposal facilities in the Los Alamos National Laboratory.* Los Alamos, USA: Los Alamos National Laboratory.

Trainer FW. 1974. Ground water in the southwestern part of the Jemez Mountains volcanic region, New Mexico. In: Siemers CT, Woodward LA, Callendar JF, eds. *Field conference guidebook. 25th Annual field conference*. Ghost Ranch, North-Central NM, USA: New Mexico Geological Society, 337–345.

Trugman AT, Detto M, Bartlett MK, Medvigy D, Anderegg WRL, Schwalm C, Schaffer B, Pacala SW. 2018. Tree carbon allocation explains forest drought-kill and recovery patterns. *Ecology Letters* **21**: 1552–1560.

Venturas MD, Sperry JS, Hacke UG. 2017. Plant xylem hydraulics: what we understand, current research, and future challenges. *Journal of Integrative Plant Biology* **59**: 356–389.

West AG, Hultine KR, Burtch KG, Ehleringer JR. 2007a. Seasonal variations in moisture use in a piñon–juniper woodland. *Oecologia* **153**: 787–798.

West AG, Hultine KR, Jackson TL, Ehleringer JR. 2007b. Differential summer water use by *Pinus edulis* and *Juniperus osteosperma* reflects contrasting hydraulic characteristics. *Tree Physiology* **27**: 1711–1720.

West AG, Hultine KR, Sperry JS, Bush SE, Ehleringer JR. 2008. Transpiration and hydraulic strategies in a piñon-juniper woodland. *Ecological Applications* **18**: 911–927.

Williams AP, Allen CD, Macalady AK, Griffin D, Woodhouse CA, Meko DM, Swetnam TW, Rauscher SA, Seager R, Grissino-Mayer HD *et al.* 2013. Temperature as a potent driver of regional forest drought stress and tree mortality. *Nature Climate Change* **3**: 292–297.

Withington JM, Reich PB, Oleksyn J, Eissenstat DM. 2006. Comparisons of structure and life span in roots and leaves among temperate trees. *Ecological Monographs* **76**: 381–397.

Supporting Information

Additional Supporting Information may be found online in the Supporting Information section at the end of the article.

Dataset S1 Fine root data compiled for species spanning a wide range of families and life forms.

Fig. S1 Specific root length and root diameter data based on first- and second-order fine roots.

Fig. S2 Daily total precipitation and midday vapor pressure deficit for ambient, drought and heat treatments.

Fig. S3 Simulated vs observed water potentials by species, plot treatment, for predawn and midday simulations.

Fig. S4 Transpiration by species treatment for year 2016, days 61–262, using sap flux data collected at SUMO.

Fig. S5 Rhizosphere flux in the bedrock layer by species and plot treatment.

Notes S1 Data collection methods at SUMO.

Table S1 Parameters used in TREES for each species.

Table S2 Dates used to force xylem refilling by species, year and plot.

Please note: Wiley Blackwell are not responsible for the content or functionality of any Supporting Information supplied by the authors. Any queries (other than missing material) should be directed to the *New Phytologist* Central Office.

See also the Commentary on this article by Santiago, **225**: 599–600.